

Background estimation in the measurement of the top quark mass using J/ψ mesons with 13 TeV proton-proton collision data from the ATLAS experiment

Kevin Nicholas Barends

Department of Physics, University of Cape Town, Private Bag X3, Rondebosch 7701, South Africa

E-mail: brnkev010@myuct.ac.za

Abstract. High precision measurements of the top quark mass, m_t , are crucial to probe internal consistency of the Standard Model and increase the precision of predictions of processes involving top quarks. The kinematic properties of the top quark's decay products are correlated to m_t . The best current measurements are predominantly limited by uncertainties related to the reconstruction of jets. However, there is a top quark decay mode which are largely independent of the aforementioned uncertainty but require large amounts of data due to their low production rate. This decay mode includes a J/ψ meson originating from a b-hadron. Background J/ψ mesons contribute and negatively impact the mass measurement. These background contributions can be distinguished from signal J/ψ mesons by exploiting the mass of a J/ψ meson and the unique displaced decay vertex feature of b-hadrons. This paper describes a data-driven technique to determine the contributions from signal and background J/ψ mesons and highlight kinematic regions which limit the contamination of background J/ψ mesons in preparation for the large data-set that will be available at the end of the next data-taking period.

1. Introduction

The top quark's mass, m_t , is a very important quantity as it's not only the heaviest fundamental particle in the Standard Model (SM), but also plays a significant role in a number of areas in the SM as well as in physics Beyond the SM (BSM) [1–3]. The precision of m_t is crucial to probe the consistency of the SM and hence, help constrain scenarios of new physics. The current average top mass of 173.0 ± 0.4 GeV [4] (also known as the Monte Carlo mass) was determined by combining the kinematics of the top quark's decay products, i.e. jets [5] and leptons. These jets and leptons originated from a primary decay of the top quark (i.e. into a W boson and a b quark) which has a branching fraction of $95.7 \pm 3.4\%$ [4]. There are other ways to measure the top mass which utilize top quark cross section measurements [2] and different ways to quote the top mass depending on the renormalization scheme [6].

Using the kinematics of the jets relies on jet reconstruction which proved to be one of the largest sources of uncertainty in previous mass measurements [7–10]. However, there are other top quark decay signatures that depend less on jet momenta and may produce a more precise measurement of the top mass. As these signatures are very rare, their study is only now

becoming possible due to the large datasets recorded by the Large Hadron Collider (LHC) experiments. One such signature consists of a lepton originating from a W boson signatures and two oppositely charged muons decaying from a J/ψ meson which originated from the b quark. However, this signature is sensitive to lepton backgrounds originating from mis-reconstructed jets or non-prompt processes [11] and J/ψ background originating from non-top quark b-/c-hadron decays (non-prompt background J/ψ), directly from the proton-proton collision (prompt J/ψ) or random combinations of two oppositely charged muons (combinatorial background) [12].

This paper describes a data-driven technique to estimate the contribution from background J/ψ mesons in the lepton+ J/ψ top quark decay signature using proton-proton collision data at $\sqrt{s} = 13$ TeV, corresponding to an integrated luminosity of 36.1 fb^{-1} .

2. ATLAS Detector

ATLAS [13] is a general-purpose detector designed to capitalize on the full potential of the LHC [14]. The magnet system consists of a superconducting solenoid surrounding the Inner Detector (ID) and three large superconducting toroids, one barrel and two end-caps, arranged azimuthally symmetric outside the calorimeters and within the Muon Spectrometer (MS). The ID performs precise particle reconstruction and identification of the collision point over $|\eta| < 2.5$, while the calorimeters measure the energy and position of particles over $|\eta| < 4.9$. The MS surrounds the calorimeters and identifies and measures muon up to $|\eta| < 2.7$. These components are integrated with a Trigger and Data Acquisition system and a computing system which selects events which consist of high transverse momenta particles or large missing transverse energy, and stores them for further analysis.

3. Event Selection

The $\ell+J/\psi$ top quark decay signature requires the W boson to decay leptonically into either an electron or a muon, at least 2 b-tagged jets and two oppositely charged muons with an invariant mass around that of a J/ψ meson (i.e. $3096.900 \pm 0.006 \text{ MeV}$). To enhance the selection of a lepton originating from a real W boson, a quantity known as the transverse mass of the W boson, $m_{\text{T}}(\text{lepton}, E_{\text{T}}^{\text{miss}}) = \sqrt{2p_{\text{T}}(\text{lepton})E_{\text{T}}^{\text{miss}}(1 - \cos(\phi(\text{lepton}) - \phi(E_{\text{T}}^{\text{miss}})))}$, was used. This quantity combines the kinematics of the lepton and the missing transverse energy (which represents the transverse kinematics of the neutrino). The kinematic requirements to extract the $\ell+J/\psi$ top quark decay signature is summarized in Table 1, where the definitions of the different observables can be found in reference [15–18].

| Description | Kinematic criteria |
|---------------------------------------|--|
| Electron (Muon) selection | Exactly 1 lepton with $p_{\text{T}} > 25 \text{ GeV}$, $ \eta < 2.5$ $ \Delta z_0 \sin \theta < 0.5 \text{ mm}$, $ d_0 /\sigma_{d_0} < 5$ (3), Isolation Gradient |
| Jet selection | At least 2 b-tagged jets with $p_{\text{T}} > 40 \text{ GeV}$ |
| Missing transverse momentum selection | $E_{\text{T}}^{\text{miss}} > 20 \text{ GeV}$ |
| Real W boson selection | $m_{\text{T}}(\text{lepton}, E_{\text{T}}^{\text{miss}}) > 40 \text{ GeV}$ |
| J/ψ muon selection | $p_{\text{T}} > 2.5 \text{ GeV}$ if $ \eta < 1.3$, $p_{\text{T}} > 3.5 \text{ GeV}$ if $1.3 < \eta < 2.5$ |
| J/ψ selection | $p_{\text{T}} > 8.5 \text{ GeV}$, $ y < 2.1$, $2 < m(\mu^+\mu^-) < 3.6 \text{ GeV}$ |

Table 1. A table with the kinematic criteria for $t \rightarrow \ell+J/\psi$ events is shown.

4. Determination of J/ψ backgrounds

The origin of the J/ψ mesons passing the kinematic criteria in Table 1 is unknown. These J/ψ mesons could be prompt J/ψ (i.e. background), non-prompt background J/ψ , combinatorial background or they could have originated from top quark b-hadron decays (non-prompt signal).

The following section describes an approach to determine the different J/ψ mesons in $\ell+J/\psi$ events. A similar approach was described in reference [19] and may be consulted for more information.

Due to the lifetime of b-hadrons [4], b-hadrons will travel before decaying, i.e. the decay vertex will be located away from the primary vertex. Therefore, prompt and non-prompt J/ψ mesons can be distinguished by studying the position of the decay vertices. This can be done by using a pseudo-proper time variable which makes use of time dilation and length contraction since the proton bunches collide at speeds near that of light. The proper decay time of b-hadrons is related to its proper decay length through $\tau = l/v$, where l is the contracted length, v is the speed of the b-hadrons and τ is the dilated time variable. The proper decay length can be represented by its actual decay length undergoing time dilation through $l = L/\gamma$, where L is the decay distance between the primary vertex and the b-hadrons decay vertex. Therefore, the proper decay time is related to the decay distance of the b-hadrons through $\tau = L/(\gamma v)$. Using the relativistic momentum relation, i.e. $p = \gamma mv$, where m is the mass and p is the momentum of the b-hadrons, the proper decay time can be written as $\tau = Lm/p$. However, since the ATLAS detector cannot fully reconstruct the momentum of b-hadrons, a good approximation would be to use the transverse momentum (and the mass) of the J/ψ mesons coming from b-hadrons. This will also aid in approximating the decay distance description since the decay distance L can be projected onto the direction of the J/ψ mesons using the reconstructed transverse momentum. Thus, a ‘‘pseudo-proper time’’ variable τ can be used to represent the decay lifetime of b-hadrons, i.e.

$$\tau \equiv \frac{\vec{L} \cdot \vec{p}_T(J/\psi)}{p_T(J/\psi)} \frac{m_{\mu^+\mu^-}}{p_T(J/\psi)} \quad (1)$$

where \vec{L} is the displacement vector from the primary vertex to the J/ψ decay vertex and $m_{\mu^+\mu^-}$ is the reconstructed mass of the J/ψ mesons (using the invariant mass of the dimuon pair). Non-prompt J/ψ decay vertices will have a $\tau > 0$ (which represents a displaced vertex) whereas prompt J/ψ decay vertices will have a $\tau = 0$, within the position and momentum resolution of the detector.

4.1. Signal J/ψ determination

Since the invariant mass and pseudo-proper time of the J/ψ mesons can be used to distinguish signal and background prompt and non-prompt J/ψ mesons, a simultaneous two-dimensional fit was applied to these distributions to determine the individual contributions. In the invariant mass distribution, the probability density functions for the non-prompt signal and prompt J/ψ mesons were modelled by Gaussian distributions while background processes were modelled by exponential functions. In the pseudo-proper time distribution, the prompt components were modelled by the sum of a delta-function distribution and a double-sided exponential function convoluted with a Gaussian function. However, the non-prompt were modelled by an exponential function convoluted with a Gaussian function. These probability density functions were defined in reference [19] as

$$\begin{aligned}
M_{J/\psi}(m_{\mu^+\mu^-}) &= G(m_{\mu^+\mu^-}; m_{J/\psi}^{PDG}, \sigma_m) \\
T_{\text{prompt } J/\psi}(\tau) &= G(\tau; 0, \sigma_\tau) \otimes \left((1-a)\delta(\tau) + ae^{-|\tau|/\tau_0} \right) \\
T_{\text{non-prompt } J/\psi}(\tau) &= G(\tau; 0, \sigma_\tau) \otimes \left(\Theta(\tau)e^{-\tau/\tau_1} \right) \\
M_{\text{prompt bkg}}(m_{\mu^+\mu^-}) &= e^{-m_{\mu^+\mu^-}/k_0} \\
M_{\text{non-prompt bkg}}(m_{\mu^+\mu^-}) &= e^{-m_{\mu^+\mu^-}/k_1} \\
T_{\text{prompt bkg}}(\tau) &= G(\tau; 0, \sigma_\tau) \otimes \left((1-b)\delta(\tau) + be^{-|\tau|/\tau_2} \right) \\
T_{\text{non-prompt bkg}}(\tau) &= G(\tau; 0, \sigma_\tau) \otimes \left(\Theta(\tau)e^{-\tau/\tau_3} \right),
\end{aligned}$$

where $m_{J/\psi}^{PDG}$ is the mass of the J/ψ meson in the Particle Data Group (PDG, i.e. reference [4]). The a , b , σ_m , σ_τ , k_i and τ_i are nuisance parameters with limits designed to produce a convergence. The total probability density function was defined in reference [19] as

$$\begin{aligned}
P_{\text{total}}(m_{\mu^+\mu^-}, \tau) &= N_{\text{signal } J/\psi} [N_{\text{prompt } J/\psi} M_{J/\psi}(m_{\mu^+\mu^-}) T_{\text{prompt } J/\psi}(\tau) \\
&\quad + (1 - N_{\text{prompt } J/\psi}) M_{J/\psi}(m_{\mu^+\mu^-}) T_{\text{non-prompt } J/\psi}(\tau)] \\
&\quad + (1 - N_{\text{signal } J/\psi}) [N_{\text{prompt bkg}} M_{\text{prompt bkg}}(m_{\mu^+\mu^-}) T_{\text{prompt bkg}}(\tau) \\
&\quad + (1 - N_{\text{prompt bkg}}) M_{\text{non-prompt bkg}}(m_{\mu^+\mu^-}) T_{\text{non-prompt bkg}}(\tau)]
\end{aligned} \tag{2}$$

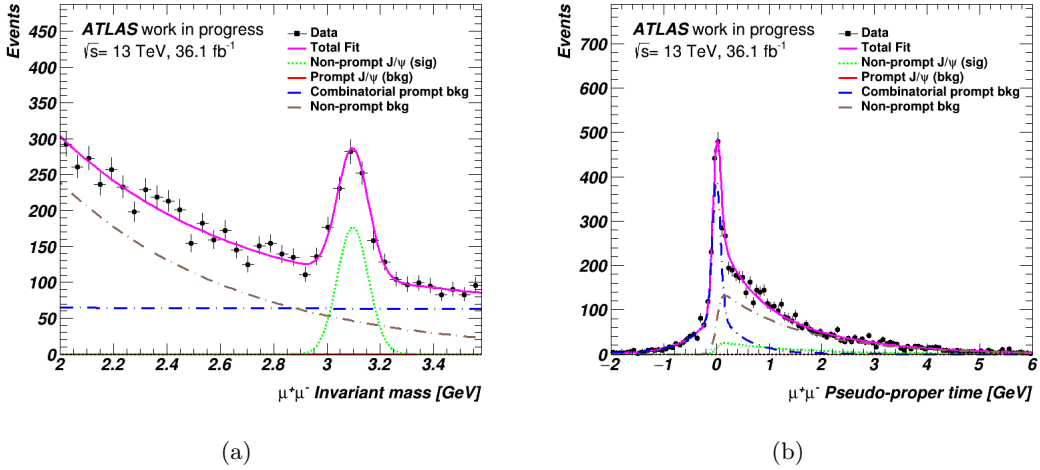


Figure 1. The invariant mass (a) and pseudo-proper time (b) distribution of the dimuon pair with the contributions from each individual process as well as the total contribution. The prompt J/ψ contribution comes out to be very small and can be seen by the red projections.

After fitting the total probability density function, the total and individual fit results in the invariant mass and pseudo-proper time distributions of the selected J/ψ mesons can be seen in Figure 1 (a) and (b), respectively. In the invariant mass distribution, the peak around the J/ψ mass is dominated by non-prompt signal J/ψ mesons with an almost negligible contribution from prompt J/ψ mesons. There are, however, sizeable contributions from both prompt and non-prompt background with the majority coming from the non-prompt background. In the pseudo-proper time distribution, the background contributions dominate and there is a reasonable

contribution coming from non-prompt signal J/ψ mesons. Once again, there is an almost negligible contribution from the prompt J/ψ mesons. However, these fit results show that the original mass selection between 2 GeV and 3.6 GeV is too loose and a tighter selection cut on the mass (i.e. 2.9 GeV to 3.3 GeV) should be applied as all the non-prompt signal J/ψ mesons are contained within this kinematic region. It is unclear from the pseudo-proper time distribution where to apply cuts in order to improve the signal to background ratio. This can be done, however, by looking at the ratio between the cumulative signal over the cumulative total (see Figure 2). The negative gradient in these distributions show regions where the background contribution dominates over the signal. From the results in Figure 2, selecting J/ψ mesons with a pseudo-proper time between 0.2 and 4.6 ps (i.e. the peaks), the signal to background ratio could improve.

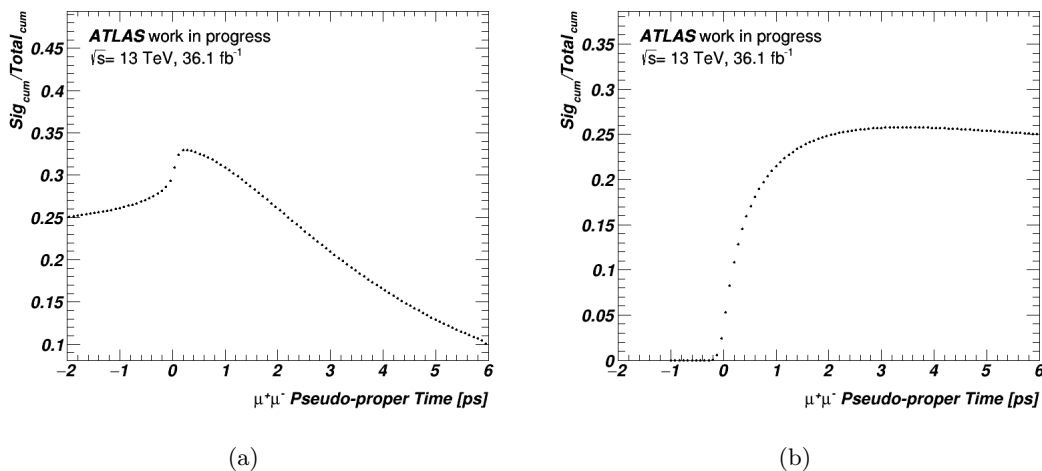


Figure 2. The ratio between the cumulative signal over the cumulative total is shown for accumulating from left to right (a) and right to left (b) as a function of pseudo-proper time. The peaks occur at 0.2 ps and 4.6 ps, respectively.

4.2. J/ψ background reduction

From the results in Figure 1 and 2, tighter selection criteria on the J/ψ mesons should improve the signal to background ratio. The invariant mass distribution of the J/ψ mesons before, (a), and after, (b), applying a tighter pseudo-proper time selection on the is shown in Figure 3. The signal to background ratio can be quantified by using $S/\sqrt{S+B}$, where S is the non-prompt J/ψ contribution and $S+B$ is the total contribution. Using the yields determined from the fits, this quantity is 0.40 before the pseudo-proper time cut and 0.58 after. Thus, showing an improvement in the signal to background ratio.

5. Conclusion

Measuring the (Monte Carlo) mass of the top quark using the $\ell+J/\psi$ decay signature reduces the dependency on jet reconstruction. However, this signature consists of background which originates from non-prompt or misidentified jets (i.e. lepton background) and from random muon pairings, b-hadron decays not originating from top quarks, or directly from the proton-proton collision (i.e. J/ψ background). This J/ψ background was determined using a data-driven technique which capitalized on the mass of the J/ψ and the displaced decay vertex of b-hadrons.

The results showed that the extracted $\ell+J/\psi$ events were dominated by background J/ψ mesons. These top quark events therefore consist of J/ψ mesons not originating from the top

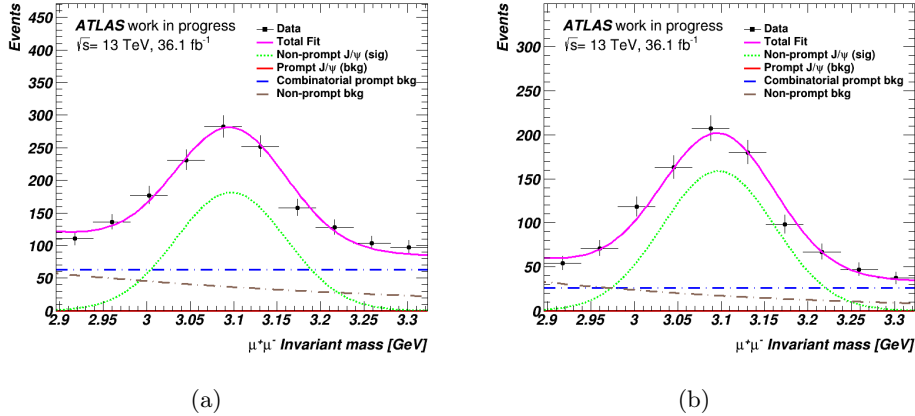


Figure 3. The invariant mass distribution of the dimuon pair in the mass window 2.9 GeV-3.3 GeV before (a) and after (b) a pseudo-proper time selection cut of $0.2 \text{ ps} < \tau < 4.6 \text{ ps}$ was applied. In each distribution, the contributions from the individual processes as well as the total contribution is shown. The prompt J/ψ contribution comes out to be very small and can be seen by the red projection.

quark’s primary decay, reducing the precision of the top mass measurement. However, the results from this data-driven technique showed kinematic regions where these background contributions could be significantly reduced (i.e. $2.9 \text{ GeV} < m_{\mu^+\mu^-} < 3.3 \text{ GeV}$ and $0.2 \text{ ps} < \tau < 4.6 \text{ ps}$). After applying these tighter selection cuts on the J/ψ mesons, the signal to background ratio improved which should result in a more precise mass measurement.

6. Acknowledgements

I would like to thank the NRF for their financial support and Dr Sahal Yacoob, Prof. Peter Onyisi and Assist. Prof. Tim Andeen for their guidance and continuous support.

7. References

- [1] Heinemeyer S, Kraml S, Porod W and Weiglein G 2003 *JHEP* **09** 075 (*Preprint hep-ph/0306181*)
- [2] Cortiana G 2016 *Rev. Phys.* **1** 60–76 (*Preprint 1510.04483*)
- [3] Degrassi G, Di Vita S, Elias-Miro J, Espinosa J R, Giudice G F, Isidori G and Strumia A 2012 *JHEP* **08** 098 (*Preprint 1205.6497*)
- [4] Patrignani C *et al.* (Particle Data Group) 2016 *Chin. Phys.* **C40** 100001
- [5] Seymour M H 1995 *AIP Conf. Proc.* **357** 568–587. 20 p URL <https://cds.cern.ch/record/283896>
- [6] Melnikov K and Ritbergen T v 2000 *Phys. Lett.* **B482** 99–108 (*Preprint hep-ph/9912391*)
- [7] Sirunyan A M *et al.* (CMS) 2017 *Eur. Phys. J.* **C77** 354 (*Preprint 1703.02530*)
- [8] Aaboud M *et al.* (ATLAS) 2016 *Phys. Lett.* **B761** 350–371 (*Preprint 1606.02179*)
- [9] Khachatryan V *et al.* (CMS) 2016 *Phys. Rev.* **D93** 072004 (*Preprint 1509.04044*)
- [10] Tevatron E W G and Aaltonen T (CD and D0) 2016 (*Preprint 1608.01881*)
- [11] Aad G *et al.* (ATLAS) 2014 URL <https://cds.cern.ch/record/1951336>
- [12] Aad G *et al.* (ATLAS) 2015 URL <https://cds.cern.ch/record/2046216>
- [13] Aad G *et al.* (ATLAS) 2008 *JINST* **3** S08003
- [14] Voss R and Breskin A (eds) 2009 *The CERN Large Hadron Collider, accelerator and experiments* URL <http://www-spires.fnal.gov/spires/find/books/www?cl=QC787.P73C37::2009>
- [15] Aad G *et al.* (ATLAS) 2016 URL <http://cds.cern.ch/record/2157687>
- [16] Aad G *et al.* (ATLAS) 2016 *Eur. Phys. J.* **C76** 292 (*Preprint 1603.05598*)
- [17] Cacciari M, Salam G P and Soyez G 2008 *JHEP* **04** 063 (*Preprint 0802.1189*)
- [18] Aad G *et al.* (ATLAS) 2015 URL <https://cds.cern.ch/record/2037697>
- [19] Aad G *et al.* (ATLAS) 2014 *JHEP* **04** 172 (*Preprint 1401.2831*)